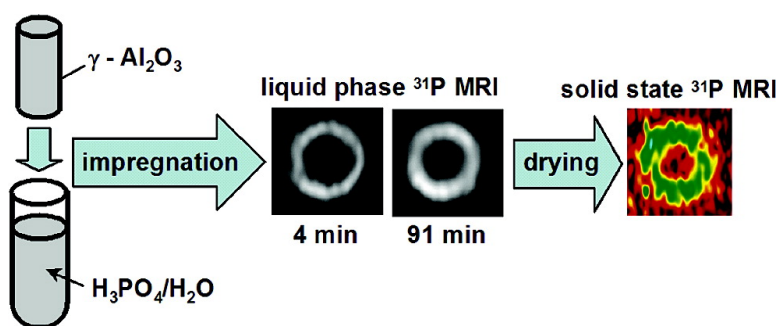Communication

Noninvasive In Situ Visualization of Supported Catalyst Preparations Using Multinuclear Magnetic Resonance Imaging

Anna A. Lysova, Igor V. Koptyug, Renad Z. Sagdeev, Valentin N. Parmon, Jaap A. Bergwerff, and Bert M. Weckhuysen

More About This Article

Additional resources and features associated with this article are available within the HTML version:

- Supporting Information
- Links to the 8 articles that cite this article, as of the time of this article download
- Access to high resolution figures
- Links to articles and content related to this article
- Copyright permission to reproduce figures and/or text from this article

View the Full Text HTML

Noninvasive In Situ Visualization of Supported Catalyst Preparations Using Multinuclear Magnetic Resonance Imaging

Anna A. Lysova,*,[†,‡] Igor V. Koptyug,[†] Renad Z. Sagdeev,[†] Valentin N. Parmon,[‡]
Jaap A. Bergwerff,[§] and Bert M. Weckhuysen[§]

International Tomography Center, 3A Institutskaya Street, Novosibirsk 630090, Russia, Boreskov Institute of Catalysis, 5 Acad. Lavrentiev Pr., Novosibirsk 630090, Russia, and Department of Inorganic Chemistry and Catalysis, Debye Institute, Utrecht University, Sorbonnelaan 16 3508 TB Utrecht, The Netherlands

Received May 27, 2005; E-mail: lysova@tomo.nsc.ru

Many technological applications use composite materials comprising an active component dispersed in a porous matrix. In particular, supported catalysts are often prepared by impregnation of a porous support using a solution of an appropriate precursor, with subsequent drying and further processing to convert the precursor into the desired active phase.[1] As the efficiency of the final catalytic system depends on both the nature and distribution of the active phase, control of the preparation process is essential.[2] The final distribution of the active component over the porous support is governed by a combination of physical and chemical processes.[3] For instance, the strength of interaction of the precursor with the support is a critical parameter. For components that strongly adsorb on the surface, a uniform distribution in the entire support can be very difficult to achieve during impregnation, while outward migration of the liquid phase can lead to a substantial redistribution of weakly adsorbed components during the drying stage.[3] The required final distribution is not always the uniform one (e.g., eggshell, egg-white, and egg-yolk) and depends on the particular application of the material. In situ characterization is essential to control the precursor transport within the support during catalyst preparation. Although this can be achieved by analysis of bisected catalyst bodies at the different stages of their preparation,[4] one would prefer to monitor these processes in a noninvasive manner.

The spectroscopic modality of nuclear magnetic resonance (NMR) is widely employed in catalytic applications and yields information about molecular scale composition, structure, and processes, albeit averaged over the entire sample. Its imaging modality (MRI) can provide essentially the same information, but with the spatial resolution on the order of tens or hundreds of microns.[5,6] The technique is noninvasive, nondestructive, and chemically specific. Therefore, MRI can be appropriate for the characterization of a wide variety of materials and dynamic processes which exhibit heterogeneity on a macroscale as often encountered in chemical engineering and heterogeneous catalysis. However, applications of MRI in heterogeneous catalysis reported to date are scarce, and many important areas of such applications remain hardly addressed. An MRI-based approach was used previously to visualize the redistribution dynamics of Pt during the impregnation of alumina pellets with H_2PtCl_6 aqueous solution.[7] This is usually the first step in the preparation of Pt/Al_2O_3 catalysts applied in hydrogenation reactions.[1] The presence of the Pt complexes changes the relaxation time of the protons of a liquid inside a porous matrix. By obtaining ^{1}H images using a relaxation contrast, the distribution of Pt inside the Al_2O_3 pellet can be derived in an indirect way. The possibility to detect the NMR signal of other nuclei with nonzero spin allows one to perform a direct in situ visualization of supported catalyst preparation. The MRI approach presented in this paper allows one to directly monitor the distribution of various nuclei inside a single catalyst body throughout the preparation process without interfering with the processes that are studied.

All imaging experiments were performed on a Bruker Avance DRX 300 MHz spectrometer equipped with imaging accessories. Impregnation was carried out on cylindrical γ-Al_2O_3 pellets, 3.2 mm in diameter and 12 mm long. The pore volume of the material was 0.43 mL/g, while its surface area was 180 m^2/g, typical values for industrial γ-Al_2O_3. Two-dimensional imaging was performed using a two-pulse spin−echo sequence in the plane transverse to the sample axis without slice selection.

As a proof of principle, the impregnation of an Al_2O_3 pellet with a 0.76 M aqueous solution of H_3PO_4 was followed using ^{1}H and ^{31}P MRI. Phosphate is present in the impregnation solutions used for the preparation of different catalytic systems, such as supported vanadium phosphate catalysts applied in selective oxidation reactions,[8] and phosphate-promoted (Ni/Co)Mo/Al_2O_3 catalysts used for hydrotreating processes.[9] Especially when acidic solutions are used, it is difficult to obtain a homogeneous distribution of phosphate, due to its strong interaction with the Al_2O_3 surface.

In Figure 1, ^{1}H and ^{31}P images detected just after the immersion of a dry pellet into the impregnation solution are presented. The ^{1}H image (Figure 1a) demonstrates that capillary action leads to very fast permeation of water into the pellet, and the ^{1}H signal of the same intensity is detected in the entire pellet after 250 s. The bright outer ring corresponds to liquid outside the pellet. The ^{31}P image (Figure 1b) detected just after the ^{1}H image demonstrates that transport of the phosphate falls far behind. The fact that the phosphate is not transported together with water into the empty pellet unequivocally demonstrates its strong interaction with the alumina surface. Adsorption of phosphate is reported to take place on basic hydroxyl groups and coordinatively unsaturated Al^{3+} sites on the Al_2O_3 surface.[9]

In a subsequent experiment, a single γ-Al_2O_3 pellet, saturated with water, was placed in a cylindrical NMR sample tube (4.2 mm i.d.) containing the H_3PO_4 solution. Figure 2 shows the resulting sequence of images detected using the ^{31}P NMR signal. The signal of the liquid phase outside the pellet was substantially reduced because of the fast repetition rate of the imaging pulse sequence to optimize sensitivity for the intra-pellet volume. The sequence of images detected clearly reveals the dynamics of $H_xPO_4^{(3−x)−}$ penetration into the pellet. It also illustrates that a single pellet can be used to monitor the complete impregnation process, as bisecting of the pellet before analysis is not necessary. A uniform distribution of the phosphate in the entire pellet is only achieved after about 14 h of impregnation, far beyond aging times typically applied in industrial catalyst preparation.

It should be noted that images in Figure 2 reflect the concentration of phosphate in the liquid phase only, while the signal of the

† International Tomography Center.
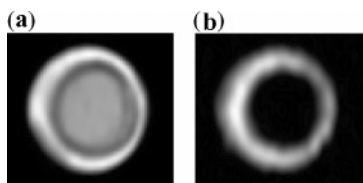‡ Boreskov Institute of Catalysis.
§ Utrecht University.

Figure 1. ^1H (a) and ^{31}P (b) images detected 250 s after immersion of a dry Al_2O_3 pellet in an aqueous solution of H_3PO_4. Bright outer ring in (a) corresponds to liquid outside the pellet.
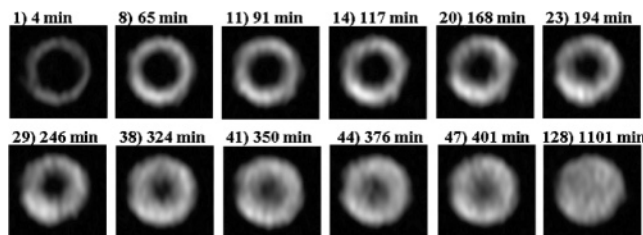

Figure 2. Dynamics of the impregnation of the γ-Al_2O_3 pellet with H_3PO_4 solution. ^{31}P images were detected with 172×371 μm^2 spatial resolution and 8 min 38 s acquisition time per image. Selected images are shown.
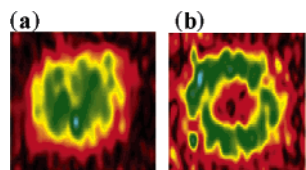

Figure 3. Two-dimensional ^{31}P images showing phosphate distribution in dried Al_2O_3 pellets. Images were detected after impregnation for 18.5 h (a) and 95 min (b). The images were acquired with 114×247 μm^2 spatial resolution in 18 h (a) and 23 h (b).

adsorbed phosphate is too low to be observable under these experimental conditions. This raises the question whether imaging of the phosphate in the liquid phase is useful for the visualization of the adsorbed species distribution. To verify this, the next impregnation MRI experiment was terminated after 95 min, well before the phosphate had time to span the entire cross-section of the pellet. The last image detected before the termination of the process was very similar to image 11 (91 min) in Figure 2. Pellets from both experiments were dried and subsequently imaged using the ^{31}P NMR signal of the solid phase.

Despite the low signal-to-noise ratio that could be achieved even with a substantially increased imaging time, the images in Figure 3 leave no doubts that adsorbed phosphate is present in the entire pellet, when it is dried 18.5 h after the start of the experiment, while termination of the impregnation process after 95 min has led to an "egg-shell"-type distribution. Comparison of the liquid phase and solid phase MRI results thus confirms the correlation of the phosphate distribution in the liquid phase during impregnation and the phosphate adsorbed on the support. Moreover, it is illustrated that the technique can be applied throughout the preparation process of supported catalyst bodies. Besides phosphate, organic chelating agents are frequently added to impregnation solutions.[11] They are found to increase the dispersion of the metal phase and the activity of (Ni/Co)Mo hydrodesulfurization catalysts, although their exact function is often not known. The role of these additives could be studied using ^{13}C MRI of ^{13}C-enriched compounds.

If the metal atom in the impregnation solution is in a diamagnetic state, it can be feasible to monitor its transport by the detection of the NMR signal of the metal atom itself. Figure 4 demonstrates such a possibility for ^{195}Pt during impregnation of a γ-Al_2O_3 pellet with an aqueous solution of H_2PtCl_6. Due to the strong interaction between the Pt complex and the Al_2O_3 surface, impregnation with
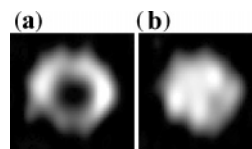

Figure 4. ^{195}Pt images detected during impregnation of the γ-Al_2O_3 pellet with an aqueous solution of H_2PtCl_6 14 min (a) and 70 min (b) after pellet immersion. ^{195}Pt images were detected with 323×698 μm^2 spatial resolution and 28 min acquisition time per image.

H_2PtCl_6 solutions generally results in the formation of egg-shell catalysts.[12] In this case, however, this effect was less pronounced because of the high precursor concentration used to improve the S/N ratio. Optimization of acquisition parameters and utilization of higher magnetic fields should allow one to successfully image ^{195}Pt and other metal ions (e.g., $^{51}V^{5+}$, $^{53}Cr^{6+}$, $^{95}Mo^{6+}$). For precursors with paramagnetic metal atoms, direct imaging is not feasible. In such cases, however, an indirect approach, based on the influence of paramagnetic species on the ^1H NMR signal of the solvent, can be used. The inhomogeneous distribution of paramagnetic cations inside a pellet saturated with water can be monitored, as was demonstrated previously for $Cu(NO_3)_2/Al_2O_3$.[13]

The multinuclear MRI technique outlined above allows one to monitor the transport of different components of the impregnation solution, as the distribution of the solvent, the metal precursor, and possible additives can all be monitored. Therefore, we believe that the MRI-based strategies, in combination with NMR signal detection of other magnetic nuclei, can be extremely useful for noninvasive visualization of the preparation of catalysts and other supported materials.

References

(1) Ertl, G.; Knözinger, H.; Weitkamp, J. *Preparation of Solid Catalysts*; Wiley-VCH: Weinheim, Germany, 1999.
(2) (a) Bell, A. T. *Science* **2003**, *299*, 1688−1691. (b) Schlögl, R.; Abd Hamid, S. B. *Angew. Chem., Int. Ed.* **2004**, *43*, 1628−1637.
(3) (a) Lee, S. Y.; Aris, R. *Catal. Rev.-Sci. Eng.* **1985**, *27*, 207−340. (b) Lekhal, A.; Glasser, B. J.; Khinast, J. G. *Chem. Eng. Sci.* **2001**, *56*, 4473−4487. (c) Neimark, A. V.; Kheifez, L. I.; Fenelonov, V. B. *Ind. Eng. Chem. Prod. Res. Dev.* **1981**, *20*, 439−450.
(4) (a) Bergwerff, J. A.; Visser, T.; Leliveld, B. R. G.; Rossenaar, B. D.; de Jong, K. P.; Weckhuysen, B. M. *J. Am. Chem. Soc.* **2004**, *126*, 14548−14556. (b) Van de Water, L. G. A.; Bergwerff, J. A.; Nijhuis, T. A.; de Jong, K. P.; Weckhuysen, B. M. *J. Am. Chem. Soc.* **2005**, *127*, 5024−5025.
(5) Callaghan, P. T. *Principles of Nuclear Magnetic Resonance Microscopy*; Clarendon Press: Oxford, 1995.
(6) (a) Koptyug, I. V.; Sagdeev, R. Z. *Russ. Chem. Rev.* **2002**, *71*, 593−617. (b) Koptyug, I. V.; Sagdeev, R. Z. *Russ. Chem. Rev.* **2003**, *72*, 165−191.
(7) Khitrina, L. Yu.; Koptyug, I. V.; Pakhomov, N. A.; Sagdeev, R. Z.; Parmon, V. N. *J. Phys. Chem. B* **2000**, *104*, 1966−1970.
(8) (a) Centi, G. *Catal Today* **1993**, *16*. (b) Roy, M.; Gubelmann Bonneau, M.; Ponceblanc, H.; Volta J. C. *Catal. Lett.* **1996**, *42*, 93−97.
(9) (a) Iwamoto, R.; Grimblot, J. *Adv. Catal.* **2000**, *44*, 417−503. (b) Sun, M. Y.; Nicosia, D.; Prins, R. *Catal. Today* **2003**, *86*, 173−189.
(10) (a) Van Veen, J. A. R.; Hendriks, P. A. J. M.; Romers, E. J. G. M.; Andrea, R. R. *J. Phys. Chem.* **1990**, *94*, 5275−5282. (b) Kraus H.; Prins, R. *J. Catal.* **1996**, *164*, 251−259.
(11) (a) Van Dillen, A. J.; Terörde, R. J. A. M.; Lensveld, D. J.; Geus, J. W.; de Jong, K. P. *J. Catal.* **2003**, *216*, 257−264. (b) Medici, L.; Prins, R. *J. Catal.* **1996**, *163*, 28−37.
(12) (a) Spieker, W. A.; Regalbuto, J. R. *Chem. Eng. Sci.* **2001**, *56*, 3491−3504. (b) Spieker, W. A.; Liu, J.; Hao, X.; Miller, J. T.; Kropf, A. J.; Regalbuto, J. R. *Appl. Catal. A* **2003**, *243*, 53−66.
(13) Koptyug, I. V.; Khitrina, L. Yu.; Parmon, V. N.; Sagdeev, R. Z. *Magn. Reson. Imaging* **2001**, *19*, 531−534.

JA053456V